Chemistry and Structure Elucidation of the Kedarcidin Chromophore

John E. Leet,* Daniel R. Schroeder, David R. Langley, Kimberly L. Colson, Stella Huang, Steven E. Klohr, Mike S. Lee, Jerzy Golik, Sandra J. Hofstead, Terrence W. Doyle, and James A. Matson

Contribution from Bristol-Myers Squibb Pharmaceutical Research Institute, Wallingford, Connecticut 06492

Received April 12, 1993

Abstract: Kedarcidin, a new chromoprotein antitumor antibiotic, was isolated from the fermentation broth of a novel actinomycete strain. Kedarcidin consists of a water-soluble apoprotein and a solvent-extractable, cytotoxic, and highly unstable chromophore. The chromophore is a new member of the enediyne class of antitumor agents. Details of the structure elucidation of kedarcidin chromophore (**1**, $C_{53}H_{60}N_3O_{16}Cl$), using a combination of NMR techniques, mass spectrometry, chemical degradation, derivatization, and sodium borohydride reduction experiments, are reported. Acidic methanolysis of **1** afforded three products: methyl α-L-mycaroside (**2**), the methyl α-glycoside of the novel amino sugar kedarosamine (**3**, $C_9H_{19}NO_3$), and a 2'-chloroazatyrosyl naphthoamide fragment (**4**, $C_{25}H_{27}N_2O_8Cl$). The presence of a reactive 8,9-epoxybicyclo[7.3.0]dodecadienediyne core was established from heteronuclear NMR and sodium borohydride reduction experiments. The nine-membered enediyne core underwent rapid aromatization upon reduction with sodium borohydride to a cyclopentyl-indene ring system. This reduction was shown to be stereospecific using sodium borodeuteride. The absolute stereochemistry of the aglycone was inferred through a combination of NMR NOE and molecular modeling data. A mechanism of action is proposed, whereby the enediyne core is activated by chemical reduction followed by spontaneous cyclization to a diradical intermediate, the species believed to cause DNA damage.

Introduction

In our search for new lead drug substances from fermentation sources, we have discovered a number of cytotoxic antitumor antibiotics which belong to the enediyne class of antitumor agents.[1,2] These molecules are characterized as being highly potent, very active in murine tumor models and active in human tumor xenografts. They also show good cytotoxicity in resistant tumor cell lines. Furthermore, the mechanism by which these agents act on DNA is unique to this class.[3] To date, four examples of this class have been described in the literature: esperamicin,[1] dynemicin,[2] calicheamicin[4] and neocarzinostatin.[5] The first three are readily extracted into organic solvents from fermentation broth. Neocarzinostatin is a chromoprotein antitumor antibiotic consisting of a 1:1 complex of a separable apoprotein and a cytotoxic non-protein chromophore. Other examples of DNA-damaging chromoproteins such as maduropeptin,[6] actinoxanthin,[7] macromomycin[8a-d] (auromomycin[8e,f]), and C-1027[9] have appeared in the literature. With the exception of neocarzinostatin,[5] and to a limited degree macromomycin[8f] and C-1027,[9b] very little has been reported on the structures of their respective chromophores. Only recently, with the advent of new NMR pulsing techniques, have the structures of C-1027[9d,e] and maduropeptin chromophores[6b] also been elucidated.

(1) (a) Golik, J.; Clardy, J.; Dubay, G.; Groenewald, G.; Kawaguchi, H.; Konishi, M.; Krishnan, B.; Ohkuma, H.; Saitoh, K.; Doyle, T. W. *J. Am. Chem. Soc.* **1987**, *109*, 3461-3462. (b) Golik, J.; Dubay, G.; Groenewald, G.; Kawaguchi, H.; Konishi, M.; Krishnan, B.; Ohkuma, H.; Saitoh, K.; Doyle, T. W. *J. Am. Chem. Soc.* **1987**, *109*, 3462-3464. (c) Golik, J.; Krishnan, B.; Doyle, T. W.; VanDuyne, G.; Clardy, J. *Tetrahedron Lett.* **1992**, *33*, 6049-6052.

(2) (a) Konishi, M.; Ohkuma, H.; Matsumoto, K.; Tsuno, T.; Kamei, H.; Miyaki, T.; Oki, T.; Kawaguchi, H.; VanDuyne, G. D.; Clardy, J. *J. Antibiot.* **1989**, *42*, 1449-1452. (b) Konishi, M.; Ohkuma, H.; Tsuno, T.; Oki, T.; VanDuyne, G. D.; Clardy, J. *J. Am. Chem. Soc.* **1990**, *112*, 3715-3716. (c) Langley, D. R.; Doyle, T. W.; Beveridge, D. L. *J. Am. Chem. Soc.* **1991**, *113*, 4395-4403.

(3) For a review on the enediyne antitumor agents, see: Nicolaou, K. C.; Dai, W.-M. *Angew. Chem., Int. Ed. Engl.* **1991**, *30*, 1387-1416.

(4) (a) Lee, M. D.; Dunne, T. S.; Siegal, M. S.; Chang, C. C.; Morton, G. O.; Borders, D. B. *J. Am. Chem. Soc.* **1987**, *109*, 3464-3466. (b) Lee, M. D.; Dunne, T. S.; Chang, C. C.; Ellestad, G. A.; Siegal, M. M.; Morton, G. O.; McGahren, W. J.; Borders, D. B. *J. Am. Chem. Soc.* **1987**, *109*, 3466-3468. (c) Lee, M. D.; Manning, J. K.; Williams, D. R.; Kuck, N. A.; Testa, R. T.; Borders, D. B. *J. Antibiot.* **1989**, *42*, 1070-1087. (d) Lee, M. D.; Dunne, T. S.; Chang, C. C.; Siegal, M. M.; Morton, G. O.; Ellestad, G. A.; McGahren, W. J.; Borders, D. B. *J. Am. Chem. Soc.* **1991**, *114*, 985-997.

(5) (a) Goldberg, I. H. *Acc. Chem. Res.* **1991**, *24*, 191-198. (b) Edo, K.; Mizugaki, M.; Koide, Y.; Seto, H.; Furihata, K.; Otake, N.; Ishida, N. *Tetrahedron Lett.* **1985**, *26*, 331-334. (c) Hensons, O. D.; Goldberg, I. H. *J. Antibiot.* **1989**, *42*, 761-768. (d) Hensons, O. D.; Giner, J.-L.; Goldberg, I. H. *J. Am. Chem. Soc.* **1989**, *111*, 3295-3299. (e) Myers, A. G.; Proteau, P. J.; Handel, T. M. *J. Am. Chem. Soc.* **1988**, *110*, 7212-7214. (f) Dedon, P. C.; Goldberg, I. H. *Biochemistry* **1992**, *31*, 1909-1917. (g) Dedon, P. C.; Jiang, Z.-W.; Goldberg, I. H. *Biochemistry* **1992**, *31*, 1917-1927. (h) Adjadj, E.; Quiniou, E.; Mispelter, J.; Favaudon, V.; Lhoste, J.-M. *Eur. J. Biochem.* **1992**, *203*, 505-511.

(6) (a) Hanada, M.; Ohkuma, H.; Yonemoto, T.; Tomita, K.; Ohbayashi, M.; Kamei, H.; Miyaki, T.; Konishi, M.; Kawaguchi, H.; Forenza, S. *J. Antibiot.* **1991**, *44*, 403-414. (b) Schroeder, D. R. Presented at the 3rd International Conference on the Biotechnology of Microbial Products, Society for Industrial Microbiology, Rohnert Park, CA, April 1993; paper S4. Manuscript in preparation.

(7) (a) Khokhlov, A. S.; Cherches, B. Z.; Reshetov, P. D.; Smirnova, G. M.; Sorokina, I. B.; Prokoptzeva, T. A.; Koloditskaya, T. A.; Smirnov, V. V.; Navashin, S. M.; Fomina, I. P. *J. Antibiot.* **1969**, *22*, 541-544. (b) Khokhlov, A. S.; Reshetov, P. D.; Chupova, L. A.; Cherches, B. Z.; Zhigis, L. S.; Stoyachenko, I. A. *J. Antibiot.* **1976**, *29*, 1026-1034.

(8) (a) Chimura, H.; Ishizuka, M.; Hamada, M.; Hori, S.; Kimura, K.; Iwanaga, J.; Takeuchi, T.; Umezawa, H. *J. Antibiot.* **1968**, *21*, 44-49. (b) Zaheer, A.; Zaheer, S.; Montgomery, R. *J. Biol. Chem.* **1985**, *260*, 11787-11792. (c) Roey, P. V.; Beerman, T. A. *Proc. Natl. Acad. Sci. U.S.A.* **1989**, *86*, 6587-6591. (d) Hidaka, T.; Yano, Y.; Yamashita, T.; Watanabe, K. *J. Antibiot.* **1979**, *32*, 340-346. (e) Yamashita, T.; Naoi, N.; Hikada, T.; Watanabe, K.; Kumada, Y.; Takeuchi, T.; Umezawa, H. *J. Antibiot.* **1979**, *32*, 330-339. (f) Kumada, Y.; Miwa, T.; Naoi, N.; Watanabe, K.; Naganawa, H.; Takita, T.; Umezawa, H.; Nakamura, H.; Iitaka, Y. *J. Antibiot.* **1983**, *36*, 200-202.

(9) (a) Otani, T.; Minami, Y.; Marunaka, T.; Zhang, R.; Xie, M.-Y. *J. Antibiot.* **1988**, *41*, 1580-1585. (b) Otani, T.; Minami, Y.; Sakawa, K.; Yoshida, K.-I. *J. Antibiot.* **1991**, *44*, 564-568. (c) Zhen, Y.; Ming, X.; Yu, B.; Otani, T.; Saito, H.; Yamada, Y. *J. Antibiot.* **1989**, *42*, 1294-1298. (d) Minami, Y.; Yoshida, K.; Azuma, R.; Saeki, M.; Otani, T. *Tetrahedron Lett.* **1993**, *34*, 2633-2636. (e) Yoshida, K.; Minami, Y.; Azuma, R.; Saeki, M.; Otani, T. *Tetrahedron Lett.* **1993**, *34*, 2637-2640. (f) Otani, T. *J. Antibiot.* **1993**, *46*, 791-802. (Note: References 9d-f are recent additions which appeared during review.)

0002-7863/93/1515-8432$04.00/0

Kedarcidin is a new chromoprotein antitumor antibiotic, produced by a novel actinomycete strain, and its fermentation, isolation, and physicochemical properties have been described elsewhere.[10] It is an acidic complex (p*I* 3.65) with an apparent molecular weight (SDS-PAGE) of 12 400 D, and it consists of an apoprotein and a cytotoxic, highly labile, non-protein chromophore. The major apoprotein is a single polypeptide chain consisting of 114 amino acid residues.[10] The chromophore is a solvent-extractable species having a molecular weight of 1029. As with neocarzinostatin, the antitumor activity of kedarcidin is due primarily to the chromophore, whereas the apoprotein is believed to play a role in the stabilization and transport of the chromophore. This paper deals with the chemistry and structure determination of the chromophore of kedarcidin (**1**).[11]

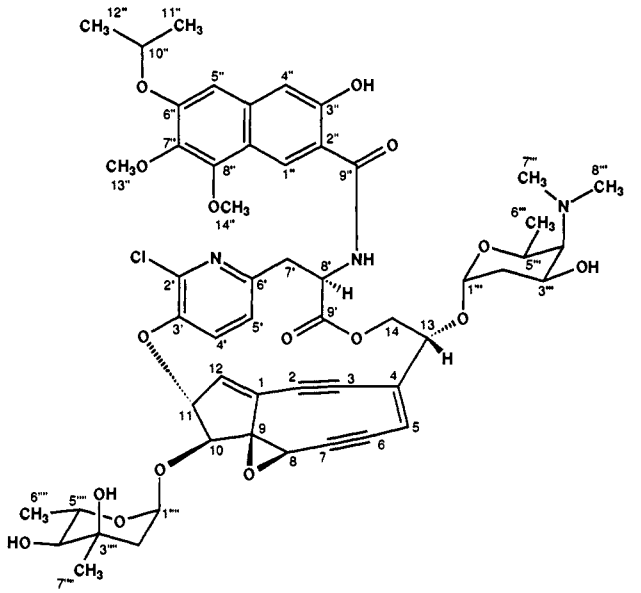

(1)

Kedarcidin was recovered from broth filtrate by absorption to a QAE anion exchanger. The purification of the chromoprotein was accomplished by gel filtration and ion-exchange chromatography.[10b] The principal bioassays used to guide the purification were the *Escherichia coli* SOS chromotest,[12] a sensitive assay used to detect DNA-damaging materials, *in vitro* cytotoxicity testing using a human colon tumor (HCT-116) cell line, and the *in vivo* P388 murine leukemia model. The presence of a non-protein chromophore in kedarcidin was first recognized from the UV spectrum, λ_{max} (H_2O) 204, 258, 306, 313 nm (log ϵ 6.09, 5.26, 4.83, 4.83). The relative ease of dissociation of the chromophore from the protein was observed using analytical reversed-phase (C-18) HPLC equipped with a photodiode array detector. In this manner, the weakly UV absorbing apoprotein eluted with the void volume, followed by a species having a distinct UV chromophore.

Kedarcidin is a varying complex depending on producing fermentation conditions. Amino acid sequencing studies on the kedarcidin apoprotein revealed the presence of three variants.[10c] The major variant polypeptide consists of 114 amino acid residues. Two minor variants were also identified; one lacks the first alanine of the major variant, and the second lacks the first two amino acids (i.e. alanine and serine) of the major variant. The ratio of apoprotein to chromophore in the kedarcidin complex also varied from lot to lot (e.g. apoprotein–chromophore molar ratio; 1:1 to 18:1), as shown by a quantitative UV method. During fermentation development and optimization studies, it was found by HPLC-UV and LC-MS that small laboratory scale (e.g. 10–35 L) fermentations employing fish meal as a media component (protein source) produced a kedarcidin complex having three chromophores of varying ratios, having molecular weights of 1029, 1015, and 1001. Pilot plant scale (e.g. 1000 L) fermentations using fish emulsion in the production media instead of fish meal produced the kedarcidin complex having only one chromophore (MW 1029). This illustrates how subtle changes in the fermentation media may influence secondary metabolite production.[13]

The crude solids containing one chromophore in the kedarcidin complex were chosen as the starting material for isolation work. Simple solvent extraction methods were explored in order to obtain a chromophore-enriched fraction for purification and characterization. The best method found to isolate this noncovalently bound chromophore was by ethyl acetate extraction of concentrated aqueous chromoprotein solution, followed by silica gel vacuum liquid chromatography using a benzene–methanol step gradient. The purified chromophore is highly unstable, as evidenced by rapid darkening of organic solutions upon solvent evaporation. Halogenated solvents such as chloroform were specifically avoided during the purification process. The compound is a buff-colored amorphous solid (SiO_2 TLC R_f 0.29, benzene–methanol, 9:2 v/v). The UV-quenching zone showed a strong zone of inhibition using SOS chromotest–TLC bioautography. The compound is highly cytotoxic (HCT-116 cell line IC_{50} 0.4 ng/mL) and shows respectable *in vivo* antitumor activity (iv implanted P388 leukemia T/C 214 at 0.25 mg/kg/dose; sc implanted B16 melanoma T/C 164 at 0.06 mg/kg/dose) in murine tumor models.

The full-scan fast atom bombardment (FAB) mass spectrum indicated that the kedarcidin chromophore (**1**) was monochlorinated with a molecular weight of 1029. The molecular formula of the kedarcidin chromophore was established as $C_{53}H_{60}N_3O_{16}Cl$ by high-resolution fast atom bombardment mass spectrometry (HRFABMS) ($[M + H]^+$ m/z 1030.3708, calcd 1030.3740), indicating 25 degrees of unsaturation in the molecule. The UV spectrum, λ_{max} (MeOH) 256, 316 nm (log ϵ 4.78, 4.16), was indicative of aromatic functionality with extended conjugation. The IR spectrum had bands (ν_{max} 3432, 1742, 1656, 1622, 2188 cm^{-1}) characteristic of hydroxyl, ester, amide, and alkyne groups, respectively. The initial ^1H- and ^{13}C-NMR data set (Table I, DMSO-d_6) revealed two *O*-methyls (δ_H 3.78, 3.95), an *N,N*-dimethylamino group (δ_H 2.45), and five *C*-methyls (δ_H 1.09–1.35), two carbonyls (δ_C 167.3, 169.1), nineteen sp^2 carbons (δ_C 102–155), four alkyne carbons (δ_C 88–104), two anomeric carbons (δ_C 94.7, 99.8), two epoxide carbons (δ_C 49.9, 71.9), four methylene carbons, ten aliphatic methines, and one aliphatic quaternary carbon. The kedarcidin chromophore therefore consists of two glycosidic units and an aglycone having aromatic, alkyne, and epoxide functionality. Our initial attempts at obtaining carbon–proton connectivity information through 2D NMR experiments

(10) (a) Lam, K. S.; Hesler, G. A.; Gustavson, D. R.; Crosswell, A. R.; Veitch, J. M.; Forenza, S.; Tomita, K. *J. Antibiot.* **1991**, *44*, 472–478. (b) Hofstead, S. J.; Matson, J. A.; Malacko, A. R.; Marquardt, H. *J. Antibiot.* **1992**, *45*, 1250–1254. (c) Hofstead, S. J.; Matson, J. A.; Lam, K. S.; Forenza, S.; Bush, J. A.; Tomita, K. U.S. Patent 5,001,112, issued March 19, 1991. (d) Zein, N.; Casazza, A. M.; Doyle, T. W.; Leet, J. E.; Schroeder, D. R.; Solomon, W.; Nadler, S. G. *Proc. Natl. Acad. Sci. U.S.A.* **1993**, *90*, 8009–8012.

(11) Leet, J. E.; Schroeder, D. R.; Hofstead, S. J.; Golik, J.; Colson, K. L.; Huang, S.; Klohr, S. E.; Doyle, T. W.; Matson, J. A. *J. Am. Chem. Soc.* **1992**, *114*, 7946–7948.

(12) (a) Quillardet, P.; Huisman, O.; D'Ari, R.; Hofnung, M. *Proc. Natl. Acad. Sci. U.S.A.* **1982**, *79*, 5971–5975. (b) Mamber, S. W.; Okasinski, W. G.; Pinter, C. D.; Tunac, J. B. *Mutat. Res.* **1986**, *171*, 83–90.

(13) Lam, K. S.; Gustavson, D. R.; Veitch, J. M.; Forenza, S.; Ross, J.; Miller, D.; Roach, J.; Lebherz, W. B.; Poole, K. Manuscript in preparation.

Table I. Kedarcidin Chromophore (**1**): ^1H and ^{13}C NMR Data (DMSO-d_6)

carbon	^{13}C ppm (mult)	^1H ppm (mult, J (Hz))	^1H–^1H NOE[a]	long-range ^1H–^{13}C correlations (COLOC)[a]
core				
1	129.0 (s)			
2	99.9 (s)			
3	99.9 (s)			
4	141.4 (s)			
5	120.1 (d)	6.19 (s)	H13, H14, H8′, H5′, H1‴	C3, C7
6	88.2 (s)			
7	104.0 (s)			
8	49.9 (d)	4.30 (br s)		C6, C7
9	71.9 (s)			
10	78.5 (d)	4.34 (d, 3.1)		C2, C9
11	83.2 (d)	5.44 (br s)	H10, H12, H1⁗	C1, C9, C3′
12	139.1 (d)	6.62 (d, 2.6)	H10, H11, H1⁗	C2, C9
13	71.9 (d)	4.53 (br s)	H5, H14, H1‴	C4, C5, C1‴
14	64.2 (t)	4.07 (d, 13.6)		C4
azatyrosine				
2′	144.5 (s)			
3′	146.3 (s)			
4′	136.2 (d)	8.05 (d, 8.3)	H8, H5′	C2′, C6′
5′	122.8 (d)	7.22 (d, 8.3)	H8, H4′, H8′	C3′
6′	155.2 (s)			
7′	37.6 (t)	a. 2.85 (m)	H7b′	C6′, C9′
		b. 3.22 (dd, 15.7, 10.7)	H7a′, H8′, NH, H5′	
8′	48.3 (d)	5.56 (m)	NH, H5, H5′, H7′, H1″	
9′	169.1 (s)			
NH		9.56 (d, 7.5)	H1″, H5′, H8′	
naphthoyl				
1″	124.0 (d)	8.48 (s)	NH	C3″, C4a″, C8″, C9″
2″	115.9 (s)			
3″	155.4 (s)			
4″	110.0 (d)	7.11 (s)	H5″, H10″	C2″, C5″, C8a″
4a″	134.3 (s)			
5″	102.1 (d)	6.97 (s)	H4″, H10″	C4″, C6″, C7″, C8a″
6″	153.3 (s)			
7″	139.0 (s)			
8″	148.4 (s)			
8a″	117.1 (s)			
9″	167.3 (s)			
10″	70.1 (d)	4.75 (sept, 6)	H5″, H4″	
11″	21.9 (q)	1.35 (d, 5.9)		C10″
12″	21.9 (q)	1.35 (d, 5.9)		C10″
13″	60.7 (q)	3.78 (s)		C7″
14″	61.6 (q)	3.95 (s)		C8″
kedarosamine				
1‴	94.7 (d)	5.11 (d, 3.2)	H5, H13, H14	
2‴	36.4 (t)	a. 1.74 (m)		
		b. 1.92 (m)		
3‴	66.0 (d)	4.12 (m)		
4‴	64.0 (d)	2.36 (br s)		
5‴	68.9 (d)	3.95 (m)		
6‴	17.1 (q)	1.16 (d, 3.1)		C4‴, C5‴
7‴	44.4 (q)	2.45 (s)		C4‴
8‴	44.4 (q)	2.45 (s)		C4‴
mycarose				
1⁗	99.8 (d)	4.81 (d, 4.2)	H10, H11, H2⁗	C2⁗, C3⁗, C5⁗
2⁗	41.6 (t)	a. 1.74 (m)		
		b. 2.05 (d, 14.3)		C1⁗, C3⁗, C4⁗
3⁗	68.5 (s)			
4⁗	76.2 (d)	2.81 (m)		
5⁗	65.6 (d)	4.27 (m)		C1⁗
6⁗	18.3 (q)	1.16 (d, 3.1)		C4⁗, C5⁗
7⁗	27.2 (q)	1.09 (s)		C2⁗, C3⁗, C4⁗

[a] Measured in 1:1 CD_3CN–DMSO-d_6 at 0 °C.

were frustrated by compound instability.[14] Thus our next approach in obtaining structural information was by chemical degradation.

Methanolysis of the Kedarcidin Chromophore (1)

The compound was readily degraded when subjected to acidic methanolysis (4.6 M HCl in methanol). Three products were isolated and characterized: methyl α-L-mycaroside (**2**), the methyl α-glycoside of the novel amino sugar kedarosamine (**3**), and the 2′-chloroazatyrosyl naphthoamide fragment (**4**).

From a mixture of α- and β-methyl glycosides of an unknown sugar species in the crude methanolysate, the major anomer (**2**) was isolated and characterized. The NMR data for compound **2** revealed a methyl α-glycoside of a 2,6-dideoxyhexopyranose. The configurations of three ring substituents were established through COSY and selective 1D proton decoupling experiments. A large ^1H–^1H coupling (J = 9.7 Hz) between H-4 and H-5 indicated a diaxial relationship; the hydroxyl and methyl groups

(14) The kedarcidin chromophore degraded rapidly (e.g. within a 1-h period) in chloroform, benzene, methanol, and DMSO solutions at ambient temperature, as evidenced by sample darkening, precipitation, and deterioration of deuterium signal lock. Approximate $t_{1/2}$ was 9 h at 37 °C in DMSO–saline solution.

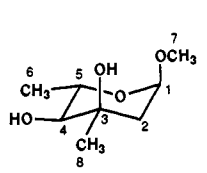

(2)

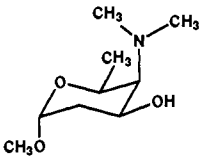

(3)

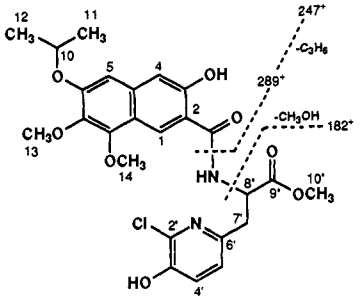

(4)

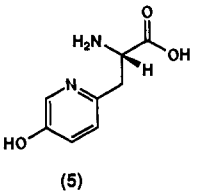

(5)

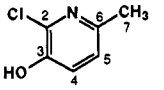

(6)

are thus equatorial. The small ^1H–^1H coupling constants (J = 3.6, 1.2 Hz) between the anomeric proton (H-1) and the adjacent methylene protons (H-2) indicated the α-anomer. The observed NMR data matched well with published data for methyl α-L-mycaroside.[15a,b] The specific rotation $[\alpha]_D$ −113° (c, 0.4, $CHCl_3$) indicated the L-configuration (lit.[15c] $[\alpha]_D$ −141° (c, 1.0, $CHCl_3$)). L-Mycarose is a component of the known macrolide antibiotics spiramycin and tylosin.[16]

The NMR data of the second methanolysis product (**3**) ($C_9H_{19}NO_3$; HRFABMS ($[M + H]^+$ m/z 190.1439, calcd 190.1443) revealed a methyl glycoside of a 2,6-dideoxyhexopyranose having an axial *N*,*N*-dimethylamino substituent (δ_H 2.59) at C-4. The small ^1H–^1H coupling (J = 3.2 Hz) between the anomeric proton (H-1) and the adjacent methylene protons (H-2) indicated the major anomer to be α. The fucopyranose configuration was determined through 2D-COSY and selective 1D proton decoupling experiments. The absolute configuration was established by X-ray crystallographic analysis of a *p*-bromobenzoate derivative.[17] This new amino sugar, designated kedarosamine, was thus established as 2,4-dideoxy-4-(dimethylamino)-L-fucopyranose.

The aromatic product (**4**) was obtained as a white powder and displayed a UV spectrum similar to that of the parent chromophore: λ_{max} (MeOH) 256, 292, 318 nm (log ϵ 4.78, 4.10, 4.05). The molecular formula of $C_{25}H_{27}N_2O_8Cl$ was established by HRFABMS ($[M + H]^+$ m/z 519.1529, calcd 519.1534), indicating 13 degrees of unsaturation. Major fragment ions were observed at m/z 289, 247, and 182. HRFABMS established the m/z 289.1078 fragment ion as $C_{16}H_{17}O_5$, the tetrasubstituted 2-naphthoyl unit as shown. Subsequent neutral loss of C_3H_6 (isopropyl) resulted in ion m/z 247.0591. A key ion at m/z 182.0010, established as $C_8H_5NO_2Cl$, is due to the 2′-chloroazatyrosine fragment with loss of methanol. In the ^1H NMR spectrum of **4** (DMSO-d_6), three aromatic singlets at δ 6.97, 7.12, and 8.56; two methoxyl groups at δ 3.80 and 3.98; and an isopropyl ether group at δ 1.34, 4.75 were assignable to the naphthyl ring. The substitution pattern about the naphthoyl moiety was determined using a series of 1D and 2D ^1H and ^{13}C correlation NMR experiments. Also evident were resonances consistent with a carbomethoxyl group (δ 3.58) and a phenolic group (δ 10.69), neither of which was present in the parent chromophore, suggesting a prior double linkage of this fragment to a central core. A pair of doublets (δ_H 7.34, 7.30, J = 8.3 Hz), a methylene signal at δ 3.03 (overlapping dd's J = 6.7, 15.9; 7.1, 15.9), a methine (δ 5.52, dd, J = 7.1, 7.9 Hz), an NH doublet (δ 9.49, J = 7.9 Hz), and the carbomethoxyl singlet were assigned to the 2′-chloroazatyrosine methyl ester portion. The trisubstitution pattern about the pyridine ring was established through direct comparisons of long-range proton–carbon couplings, one-bond coupling constants, and carbon chemical shifts with those of synthetic 2-chloro-3-hydroxy-6-methylpyridine[18] (**6**). The antibiotic azatyrosine (**5**) (L-β-(5-hydroxy-2-pyridyl)alanine)[19] has been previously obtained from *Streptomyces*. The kedarcidin chromophore is the first known example of a natural product containing this moiety as a structural fragment.

The information gained from degradation products **2**, **3**, and **4** was in agreement with the cleavages observed in the mass spectrum of the parent kedarcidin chromophore (**1**) (Figure 1). The base peak m/z 158 is due to facile cleavage of the amino sugar kedarosamine. This was confirmed by HRFABMS (m/z 158.1178, $C_8H_{16}NO_2$). A small ^1H–^1H coupling (J = 3.2 Hz) between the anomeric proton (δ 5.11) and the adjacent axial methylene proton (δ 1.74) indicated α-linkage. A weak ion at m/z 886.2940 ($C_{46}H_{49}N_3O_{13}Cl$) due to cleavage of the mycarose was also observed. The α-linkage was again apparent from the ^1H–^1H coupling constant (J = 4.2 Hz) between the anomeric proton (δ 4.81) and the adjacent axial methylene proton (δ 2.05). Major fragment ions were observed at m/z 289 and 247, as with compound **4**. The FAB parent MS/MS spectrum of the m/z 289 ion provided further substructural information and contained an abundant at m/z 505, corresponding to the chloroazatyrosyl naphthoamide substructure. The above data indicate that the kedarosamine and mycarose units are each α-linked by a single bond to a central core structure, while the naphthoyl group is linked to a 2′-chloroazatyrosyl moiety which bridges the core. The remaining central core must therefore consist of $C_{14}H_8O$, which accounts for the remaining nine sites of unsaturation in the parent molecule. The structure elucidation of this central core portion was subsequently solved through chemical reduction and low-temperature NMR experiments.

Sodium Borohydride Reduction

As previously mentioned, the kedarcidin chromophore (**1**) is very unstable once separated from the protective environment of its associated apoprotein. To obtain proton–carbon connectivity information from extended 2D NMR experiments, it became necessary to prepare a derivative that was more stable. Mild reduction was chosen as a first approach. Like the neocarzinostatin chromophore,[5c] the kedarcidin chromophore reacted vigorously with sodium borohydride. The molecular weight of 1033 was determined by FABMS. The molecular formula of the reduction product, $C_{53}H_{64}N_3O_{16}Cl$, was established by HRFABMS ($[M + H]^+$ m/z 1034,4021, calcd 1034.4053), indicating incorporation of four additional hydrogen atoms upon reduction. Reduction with sodium borodeuteride in methanol gave a mixture of products by FABMS; the major ion m/z 1035 ($[M + H]^+$) indicated incorporation of one deuterium atom. Reduction with sodium borodeuteride in deuterated methanol gave a product, $C_{53}H_{61}D_3N_3O_{16}Cl$, (HRFABMS $[M + H]^+$ m/z 1037.4210, calcd 1037.4242) indicating incorporation of three deuterium atoms. Thus, one of the deuteriums introduced upon reduction was exchanged during aqueous workup.

The ^1H-NMR spectrum (Table II) ($CDCl_3$) of the sodium borohydride reduction product revealed noticeable changes from

(15) (a) Thiem, J.; Elvers, J. *Chem. Ber.* **1978**, *111*, 3514–3515. (b) Omura, S.; Nakagawa, A.; Neszmelyi, A.; Gero, S. D.; Sepulchre, A.-M.; Piriou, F.; Lukacs, G. *J. Am. Chem. Soc.* **1975**, *97*, 4001–4009. (c) Regna, P. P.; Hochstein, F. A.; Wagner, R. L.; Woodward, R. B. *J. Am. Chem. Soc.* **1953**, *75*, 4625–4626.

(16) *Dictionary of Organic Compounds*, 5th ed.; Buckingham, J., Ed.; Chapman and Hall: New York, 1982; Vol. 4, p 4126.

(17) Leet, J. E.; Golik, J.; Hofstead, S. J.; Matson, J. A.; Lee, A. Y.; Clardy, J. *Tetrahedron Lett.* **1992**, *33*, 6107–6110.

(18) Weis, C. D. *J. Heterocycl. Chem.* **1976**, *13*, 145–147.

(19) Inouye, S.; Shomura, T.; Tsuruoka, T.; Ogawa, Y.; Watanabe, H.; Yoshida, J.; Niida, T. *Chem. Pharm. Bull.* **1975**, *23*, 2669–2677.

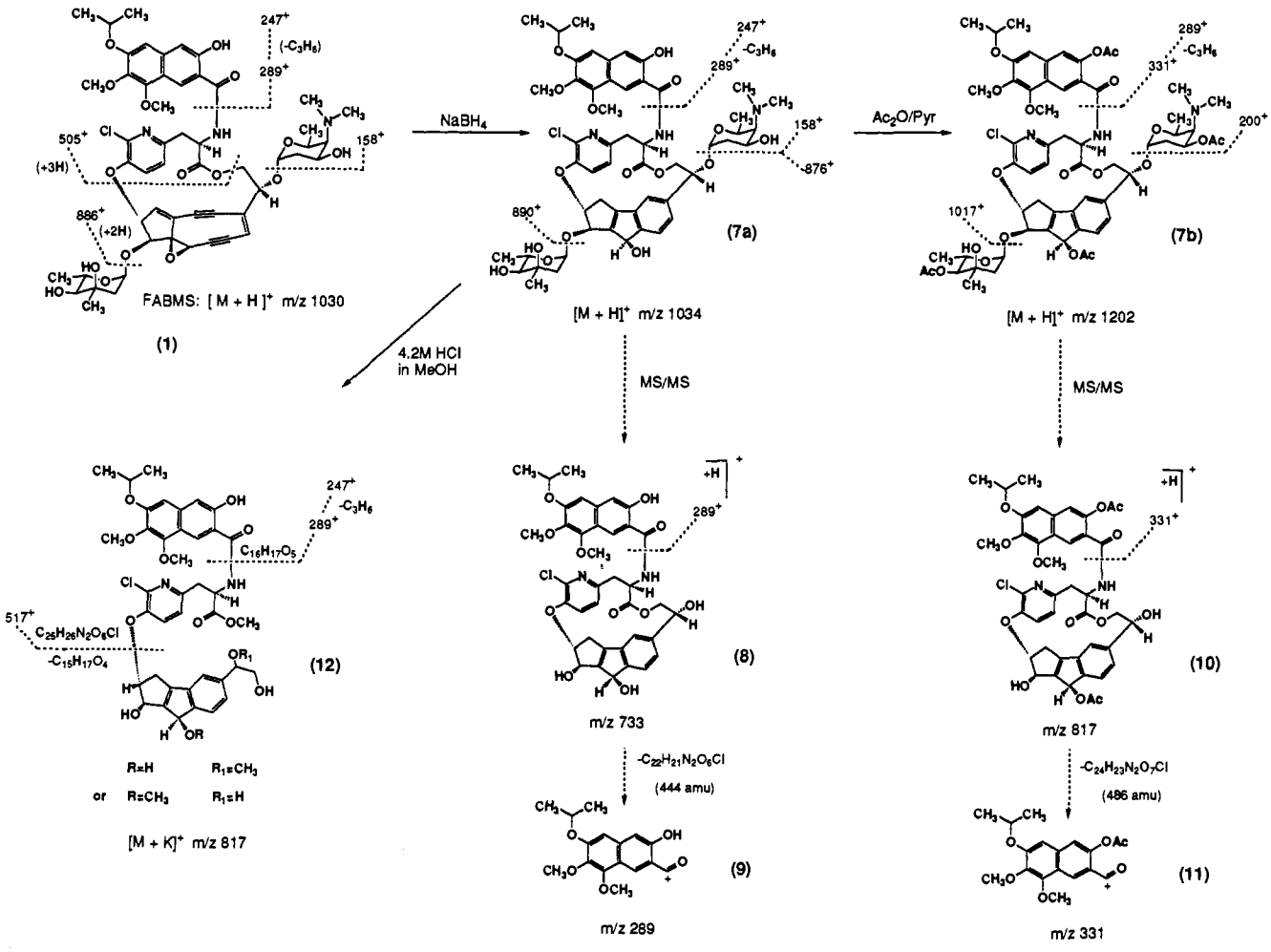

Figure 1. Summary of mass spectral fragmentations of the kedarcidin chromophore (**1**) and related derivatives.

that of the parent chromophore (Table I). These included a new ABX pattern (δ 7.40, 7.49, 6.36), consistent with a 1,2,4-trisubstituted benzenoid ring, and the disappearance of two proton signals at δ 6.19 and 6.62. Also evident was a previously unobserved geminal pair at δ 2.40 and 2.73 (J = 18.2 Hz) and a new methine at δ 5.07. Apparent in the ^{13}C-NMR spectrum was the appearance of four new olefinic resonances and loss of the alkyne resonances (δ 88–104, Table I). Only minor chemical shift changes were observed in the 2′-chloroazatyrosyl naphthoamide portion and the two glycosidic units.

Interpretation of the ^{1}H–^{1}H COSY, HETCOR, COLOC,[20] and HMBC[21] data led to the assignment of a tetrasubstituted cyclopentyl–indene ring system as the structure of the remaining core fragment (Figure 2). A significant NOE was observed between the indene methine at δ 5.07 and the two ortho protons (δ 6.68 and 7.02) on the pyridine ring, indicating close proximity between the two ring systems. The azatyrosine unit is bridged between both ends of the cyclopentyl–indene system. This was established by a three-bond heteronuclear coupling between C-3′ (δ 146.9) of the pyridine and the reduced core C-11 methine (δ 5.49). The second, crucial three-bond coupling was observed in an HMBC experiment on a tetraacetate derivative of the reduction product (Table III); this coupling was not seen in the reduction product itself. The coupling between the C-9′ carbonyl resonance of the azatyrosine portion and one of the C-14 methylene protons completes the bridge. Additionally, strong NOE's were observed between H-3 (δ 6.36) and H-13 (δ 4.44); H-5 (δ 7.40) and H-14b (δ 4.59); and H-5′ (δ 6.68) and H-8′ (δ 5.35). This defines the conformation of the azatyrosine bridge and sets the relative stereochemistry at C-13 and C-8′.

Attachment of the sugar mycarose to the reduced core was established by ^{1}H–^{13}C long-range coupling between the anomeric carbon (δ 97.7) and the core methine at C-10 (δ 5.32) and by NOE's between the anomeric proton (δ 5.43) and the C-8, C-10, and C-11 methines (δ 5.07, 5.32, and 5.49, respectively). In addition, NOE's between H-5′′′′ (δ 3.94) and H-10, H-11 were observed. Attachment of the amino sugar kedarosamine to the core was evidenced by a strong NOE interaction between its anomeric proton (δ 5.11) and the C-3, C-13 core protons (δ 6.36, 4.44). The glycosidic linkages are α, as previously identified.

Supporting evidence for the structure of reduction product **7a** was provided by MS/MS substructure analysis (Figure 1). As with the native, nonreduced chromophore, substructure ions of m/z 158, 247, 289, and 505 were observed. This further indicated that the reduction did occur on the central core. In addition, ions m/z 876 (loss of 158, kedarosamine), 890 (loss of 143, mycarose), and 733 (losses of 158 and 143, both sugars) were observed. The parent MS/MS spectrum of the m/z 289 ion (**9**) contained the m/z 733 ion, indicating that the naphthoyl moiety is part of the m/z 733 substructure (**8**).

The kedarcidin chromophore reduction product was peracetylated (**7b**). The molecular weight of 1201 was established by FABMS, indicating that four of the possible five sites were acetylated. The daughter MS/MS spectrum of the m/z 1202 $[M + H]^+$ ion exhibited a fragmentation pattern similar to that observed with the reduction product (**7a**) (Figure 1). Acetylated substructures were identified by direct comparisons of daughter MS/MS spectra for each compound. Acetylation of the naphthoyl

(20) Kessler, H.; Griesinger, C.; Zarbock, J.; Loosli, H. R. *J. Magn. Reson.* **1984**, *57*, 331–336.
(21) Bax, A.; Summers, M. F. *J. Am. Chem. Soc.* **1986**, *108*, 2093–2094.

Table II. Kedarcidin Chromophore Reduction Product (**7a**): ^{1}H- and ^{13}C-NMR Data ($CDCl_3$)

carbon	^{13}C ppm (mult)	^{1}H ppm (mult, J (Hz))	^{1}H–^{1}H NOE	long-range ^{1}H–^{13}C correlations (COLOC)
core				
1	149.3 (s)			
2	136.1 (s)			
3	117.9 (d)	6.36 (s)	H13	C1, C5, C7
4	141.1 (s)			
5	124.6 (d)	7.40 (d, 7.9)	H6, H14b	C3, C7
6	124.9 (d)	7.49 (d, 7.9)	H5, H8	C2, C4
7	148.5 (s)			
8	71.2 (d)	5.07 (br s)	H5, H6, H10, H4′, H5′, H8′, H1′′′′, H2′′′′a, H2′′′′b, H4′′′′	C1, C9
9	150.3 (s)			
10	77.6 (d)	5.32 (m)	H11, H1′′′′, H5′′′′	C1, C9, C11, C1′′′′
11	88.3 (d)	5.49 (t, 4.5)	H10, H12a, H12b, H5′′′′	C1, C9, C3′
12	29.0 (t)	a. 2.40 (d, 18.2)	H12b	C1, C9, C10, C11
		b. 2.73 (br d, 18.2)	H10, H11, H12a	C1, C9
13	75.9 (d)	4.44 (dd, 3.3, 9.5)	H3, H14b, H1′′′	C1′′′
14	65.7 (t)	a. 4.01 (dd, 3.3, 10.5)	H13, H14b, H1′′′	C4
		b. 4.59 (dd, 9.5, 10.5)	H5, H13, H14a, H1′′′	C13
azatyrosine				
2′	147.4 (s)			
3′	146.9 (s)			
4′	135.2 (d)	7.02 (d, 8.1)	H8, H5′	C2′, C6′
5′	121.1 (d)	6.68 (d, 8.1)	H4′, H8′	C3′
6′	153.5 (s)			
7′	40.1 (t)	a. 2.81 (dd, 9.9, 17.5)		C9′
		b. 2.90 (dd, 2.8, 17.5)		C6′, C9′
8′	49.0 (d)	5.35 (dd, 2.8, 9.9)	NH, H5′, H1″	
9′	168.5 (s)			
NH		7.76 (d, 7.6)	H7′, H8′, H1″	C9″
naphthoyl				
1″	121.3 (d)	8.17 (s)	NH, H7′, H8′, H14″	C3″, C4a″, C8″, C9″
2″	113.6 (s)			
3″	157.1 (s)			
4″	110.8 (d)	7.04 (s)	H5″, H10″	C2″, C3″, C5″, C8a″
4a″	135.1 (s)			
5″	101.9 (d)	6.68 (s)	H10″	C4″, C6″, C7″, C8a″
6″	154.0 (s)			
7″	139.3 (s)			
8″	148.3 (s)			
8a″	117.4 (s)			
9″	169.1 (s)			
10″	70.6 (d)	4.69 (sept, 6.0)	H4″, H5″	
11′	21.9 (q)	1.42 (d, 6.0)	H10″	C10″
12″	21.9 (q)	1.43 (d, 6.0)	H10″	C10″
13″	61.1 (q)	3.87 (s)		C7″
14″	61.6 (q)	4.09 (s)	H1″	C8″
kedarosamine				
1′′′	97.2 (d)	5.11 (br s)	H3, H13, H2′′′a, H2′′′b	C3′′′, C5′′′
2′′′	35.5 (t)	a. 1.77 (ddd, 3.9, 10.3, 14.0)	H1′′′, H2′′′b	
		b. 2.00 (ddd, 2.0, 5.7, 14.0)	H1′′′, H2′′′a	C1′′′
3′′′	63.3 (d)	3.91 (m)		
4′′′	63.8 (d)	2.39 (br s)	H3′′′, H5′′′	C2′′′, C3′′′, C7′′′, C8′′′
5′′′	68.3 (d)	3.76 (dq, 3.0, 7.0)	H3′′′, H4′′′	C6′′′
6′′′	17.7 (q)	0.98 (d, 7.0)	H5′′′	C4′′′, C5′′′
7′′′	45.0 (q)	2.52 (s)	H3′′′, H4′′′, H5′′′	C4′′′
8′′′	45.0 (q)	2.52 (s)	H3′′′, H4′′′, H5′′′	C4′′′
mycarose				
1′′′′	97.7 (d)	5.43 (d, 3.4)	H8, H10, H11, H2′′′′a, H2′′′′b	C3′′′′, C5′′′′
2′′′′	41.0 (t)	a. 1.96 (dd, 3.4, 14.6)	H1′′′′, H2′′′′b	
		b. 2.26 (d, 14.6)	H1′′′′, H2′′′′a	C1′′′′, C3′′′′, C4′′′′
3′′′′	69.6 (s)			
4′′′′	76.5 (d)	3.03 (d, 9.4)		
5′′′′	66.5 (d)	3.94 (m)	H10, H11	C1′′′′
6′′′′	18.1 (q)	1.40 (d, 6.1)	H4′′′′, H5′′′′	C4′′′′, C5′′′′
7′′′′	25.4 (q)	1.23 (s)	H2′′′′a, H2′′′′b, H4′′′′	C2′′′′, C3′′′′, C4′′′′

substructure (**9**) (m/z 289) was confirmed by the presence of the m/z 331 fragment ion (**11**). Similarly, acetylation of the kedarosamine substructure (m/z 158) was confirmed by the presence of the m/z 200 fragment ion. The abundant fragment ion observed at m/z 1017 resulted from loss of a monoacetylated mycarose substructure (186 amu). The remaining acetylated substructure was confirmed by the presence of the m/z 817 fragment ion (**10**), corresponding to a diacetylated reduced core chloroazatyrosyl naphthoamide substructure. This substructure ion results from successive losses of the acetylated mycarose and kedarosamine units. The FAB parent MS/MS spectrum of the m/z 331 naphthoyl substructure (**11**) contained the m/z 817 fragment ion (**10**) and indicated neutral loss of the monoacetylated reduced core chloroazatyrosine substructure (486 amu). In the NMR spectra, changes in chemical shifts (mycarose H-4′′′′, δ 3.03 to 4.67; kedarosamine H-3′′′, δ 3.91 to 5.27; aromatized core H-8, δ 5.07 to 6.17; naphthoyl C3″, δ 157.1 to 145.3; C2″, δ 113.6 to 123.0; C4″, δ 110.8 to 119.0) revealed acetylation at the indicated positions (**7b**). The HMBC data for the tetraacetate

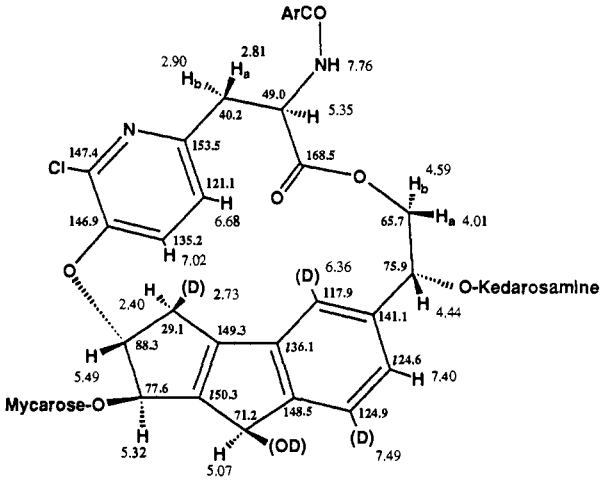

Figure 2. Kedarcidin chromophore $NaBH_4$ ($NaBD_4$) reduction product: Detail of bridged core.

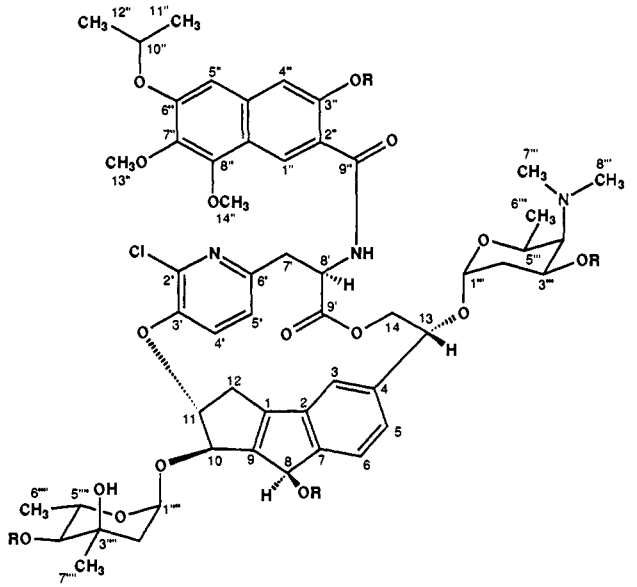

(7a, R=H)

(7b, R=Ac)

(Table III) proved to be complementary with the COLOC data for the starting reduction product (Table II).

The reduction product was subjected to acidic methanolysis. Methanolysis products **2**, **3**, and **4** were detected by TLC in the reaction mixture, as previously described. Another minor product was isolated, which by NMR revealed the loss of the mycarose and kedarosamine units and opening of the lactone (Figure 1). The molecular formula for this product (**12**) was established by HRFABMS as $C_{40}H_{43}N_2O_{12}Cl$ ([M + K]$^+$ 817.2155, calcd 817.2142). In the full-scan mass spectrum, the expected m/z 289 fragment ion due to loss of the 2-naphthoyl group was observed, as was the further loss of isopropyl, giving ion m/z 247. A key ion at m/z 517.1392 is due to the chloroazatyrosyl naphthoamide substructure $C_{25}H_{26}N_2O_8Cl$, resulting from neutral loss of the cyclopentyl–indene unit $C_{15}H_{17}O_4$.

Upon sodium borodeuteride reduction of the kedarcidin chromophore, the signals at δ 2.73, 6.36, and 7.49, present in the borohydride product, disappeared, indicating deuterium incorporation at these sites (Figure 2). The δ 7.40 doublet in turn collapsed to a singlet. This 1,4-disubstitution of a benzenoid ring with deuterium is consistent with a precursor 1,4-benzenoid

Table III. Tetraacetate of Kedarcidin Chromophore Reduction Product (7b): ^{1}H- and ^{13}C-NMR Data ($CDCl_3$)

carbon	^{13}C ppm	^{1}H ppm (mult, J (Hz))	long-range ^{1}H–^{13}C correlations (HMBC)
core			
1	152.3		
2	136.8		
3	118.0	6.36 (s)	C1, C5, C7, C13
4	141.4		
5	125.2	7.40 (br s)	C13
6	126.0	7.40 (br s)	C2, C4, C8
7	145.2		
8	70.9	6.17 (s)	C1, C7, C9, AcCO (170.5)
9	146.7		
10	79.0	5.17 (m)	C11, C1′′′′
11	88.4	5.44 (t, 4.6)	C1, C3′
12	29.2	2.43 (m)	
		2.72 (m)	
13	75.7	4.45 (dd, 3.3, 9.3)	
14	65.4	a. 3.99 (dd, 3.3, 10.4)	
		b. 4.56 (dd, 9.3, 10.4)	C9′, C4, C13
8-OAc	21.3	2.06 (s)	AcCO (170.5)
	170.5		
azatyrosine			
2′	147.3		
3′	146.7		
4′	135.4	7.11 (d, 8.1)	C2′, C3′, C6′
5′	121.4	6.70 (d, 8.1)	C3′
6′	154.0		
7′	40.1	a. 2.73 (dd, 9.7, 17.6)	C6′, C8′, C9′
		b. 2.89 (dd, 2.4, 17.6)	C6′, C9′
8′	49.8	5.34 (ddd, 2.4, 7.4, 9.7)	C6′, C9′
9′	168.5		
NH		7.75 (d, 7.4)	C9″
naphthoyl			
1″	126.0	8.59 (s)	C3″, C4a″, C8″, C9″
2″	123.0		
3″	145.3		
4″	119.0	7.34 (s)	C2″, C3″, C5″, C8a″
4a″	132.5		
5″	103.6	6.82 (s)	C4″, C6″, C7″, C8a″
6″	153.6		
7″	141.8		
8″	149.0		
8a″	121.8		
9″	164.5		
10″	70.6	4.67 (m)	
11″	21.9	1.41 (d, 6.0)	C10″
12″	21.9	1.42 (d, 6.0)	C10″
13″	61.0	3.90 (s)	C7″
14″	61.6	4.03 (s)	C8″
3″-OAc	21.5	2.40 (s)	AcCO (169.3)
	169.3		
kedarosamine			
1‴	96.7	5.12 (br s)	
2‴	32.9	a. 1.93 (m)	C1‴, C3‴, C4‴
		b. 2.17 (m)	
3‴	70.9	5.27 (m)	
4‴	61.4	2.62 (br s)	
5‴	68.2	3.72 (m)	
6‴	16.7	0.86 (d, 6.5)	C5‴
7‴	44.3	2.48 (s)	C4‴
8‴	44.3	2.48 (s)	C4‴
3‴-OAc	20.9	2.11[b] (s)	AcCO (170.8[a])
	170.8[a]		
mycarose			
1′′′′	98.7	5.19 (d, 3.8)	C10, C3′′′′, C5′′′′
2′′′′	41.5	a. 1.98 (dd, 3.8, 14.5)	
		b. 2.31 (d, 14.5)	C1′′′′, C3′′′′, C4′′′′
3′′′′	69.4		
4′′′′	77.3	4.67 (d, 10.0)	C5′′′′, AcCO (170.9)
5′′′′	63.8	4.37 (dq, 6.2, 10.0)	C3′′′′, C4′′′′
6′′′′	17.6	1.24 (d, 6.2)	C4′′′′, C5′′′′
7′′′′	25.2	1.11 (s)	C2′′′′, C3′′′′, C4′′′′
4′′′′-OAc	20.9	2.12[b] (s)	AcCO (170.9[a])
	170.9[a]		

[a,b] Values may be interchangeable.

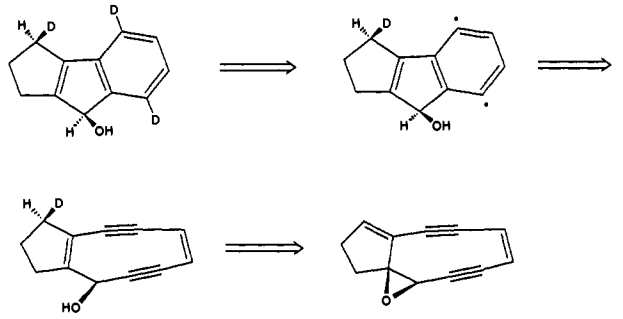

Figure 3. Retroanalysis: Aromatized core fragment.

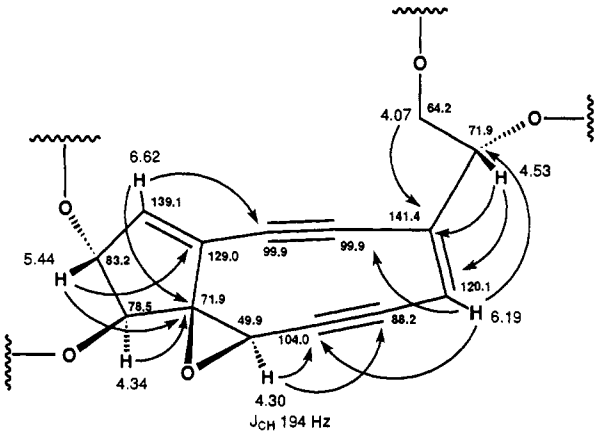

Figure 4. Kedarcidin chromophore enediyne core: Carbon–proton long-range couplings (COLOC).

diradical resulting from Bergman-type[22] aromatization of an enediyne. Since only the δ 2.73 signal of the newly formed geminal pair was deuterated, this was indicative of stereospecific attack on an sp^2 carbon with hydride/deuteride. From a retroanalysis of the reduction product, we have proposed the 8,9-epoxybicyclo-[7.3.0]dodecadienediyne system as the reactive species (Figure 3). The similarity to the C_{14} dienediyne carbon skeleton in the neocarzinostatin chromophore suggests a common biogenetic origin.[5d]

Structure of the Kedarcidin Chromophore (1)/Absolute Configuration

A complete NMR spectral data set was obtained in DMSO-d_6 for the unreduced chromophore (Table I). We later found that degradation was minimized when using 1:1 CD_3CN–DMSO-d_6 at 0 °C, allowing for extended COLOC and NOE experiments.[23] The key long-range carbon–proton couplings for the enediyne core are indicated in Figure 4. The presence of an epoxide fused to the C-8 and C-9 positions of the enediyne system was supported by a large coupling constant (J_{C-H} = 194 Hz) between C-8 (δ 49.9) and its attached proton (δ 4.30). This proton (δ 4.30) displayed a significant NOE interaction with the two ortho protons H-4′ and H-5′ (δ 8.05, 7.22) on the pyridine ring, indicating that the δ 4.30 proton resides on the same face of the dodecadienediyne ring system as the bridging pyridine moiety and establishing the relative stereochemistry of the epoxide. Additionally, a key NOE between H-8′ (δ 5.56) of the azatyrosine system and the core olefinic proton H-5 (δ 6.19) establishes the relative configuration of the C-8′ methine. Long-range couplings between H-5 (δ 6.19) and H-8 (δ 4.30) and between H-5 and H-13 (δ 4.53) were also observed. Three quarternary carbon signals at δ 88.2, 99.9 (degenerate), and 104.0 were assigned to alkyne carbons C-6,

(22) (a) Lockart, T. P.; Comita, P. B.; Bergman, R. G. *J. Am. Chem. Soc.* **1981**, *103*, 4082–4090. (b) Jones, R. R.; Bergman, R. G. *J. Am. Chem. Soc.* **1972**, *94*, 660–661. (c) Bergman, R. G. *Acc. Chem. Res.* **1973**, *6*, 25–31.

(23) CD_3CN–DMSO-d_6 (1:1) chemical shifts: ^1H values shifted +0.1 ppm; ^{13}C values shifted +2 ppm from DMSO-d_6 shifts.

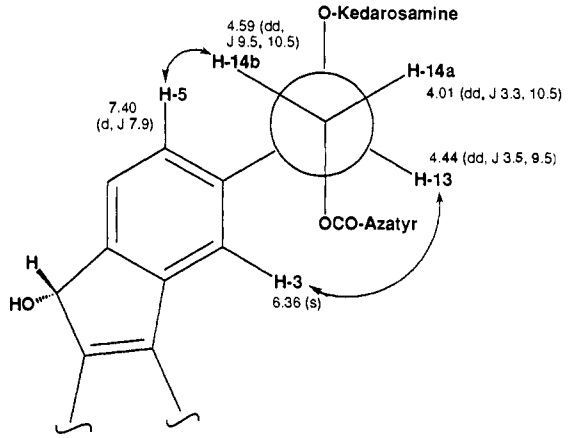

Figure 5. Newman projection showing key NOE's and relative stereochemistry of C-13 of the reduction product (**7a**). The H-13–C-13–C-14–H-14b dihedral angle is 177.63° from the model of the reduction product global minimum.

C-2, C-3, and C-7, respectively. The ^1H–^1H coupling constant (J = 3.1 Hz) between the two cyclopentenyl methines H-10 (δ 4.34) and H-11 (δ 5.44) was indicative of trans substitution, as in the neocarzinostatin chromophore.[5b,e] The relative stereochemistry of the enediyne core was thus established from ^1H–^1H coupling constants and NOE data. The structure of the kedarcidin chromophore (**1**) is thus indicated.

The reduction product (**7a**) proved instrumental in the determination of, first, the relative stereochemistry of the 2′-chloroazatyrosine-bridged cyclopentyl–indene ring system and, ultimately, the absolute stereochemistry of the kedarcidin chromophore. In the nonreduced chromophore (**1**), the greater flexibility of the [7.3.0] dodecadienediyne core gives rise to multiple energy minima (i.e. conformers). As a result, some of the observed NOE's are inconsistent with any one given minimum. Reduction and subsequent aromatization of the enediyne core, however, reduces the conformational flexibility of the azatyrosyl-bridged core system. This was denoted by the loss of several NOE's, in particular, the H-8′ (δ 5.56) to H-5 (δ 6.19) and H-13 (δ 4.53) to H-5 NOE's (Tables I and II). Two key NOE's between H-3 (δ 6.36) and H-13 (δ 4.44) and between H-5 (δ 7.40) and H-14b (δ 4.59), and a large coupling (J_{H-H} = 9.5 Hz) between vicinal protons H-13 and H-14b (i.e. anti), allowed for the assignment of relative stereochemistry at C-13 (Figure 5).

Using the CHARMM force field[24] and conformational searching routines, the global minimum for each diastereomer was determined. The 8*R*,10*S*,11*R*,13*R*,8′*R* enantiomer was found to be consistent with the NOE data set (Table II, Figure 6a). The NOE's between H-3 and H-13, H-5 and H-14b, and H-5′ and H-8′, together with the energetically favored conformation of the ester (i.e. oxygen lone pair is anti to the carbonyl), define the conformation and relative stereochemistry of the 2′-chloroazatyrosine bridge. The modeling predictions are consistent with the loss of NOE's between H-5 and H-13 and between H-5 and H-8′. This confirms the rigidity of the aromatized core system and supports the stereochemical assignments.

The assignment of absolute stereochemistry was determined on the basis of the NOE's between the L-mycarose and the aglycone. Since NOE's are obtained from dynamic molecules, it is important to evaluate the NOE's within the conformational space sampled by the diastereomers. The energetically accessible conformations were determined by grid map calculations (Figure 6b). The reference point in the grid calculations is at (0.0, 0.0), where the H-10–C-10–O-10–C-1′′′′ and C-10–O-10–C-1′′′′–H-1′′′′ dihedrals were set to zero. Only the 8*R*,10*S*,11*R*,13*R*,8′*R* enantiomer (Figure 6a) was consistent with the observed NOE's.

(24) Brooks, B. R.; Bruccoleri, R. E.; Olafson, B. D.; States, D. J.; Swaminathan, S.; Karplus, M. *J. Comput. Chem.* **1983**, *4*, 187–217.

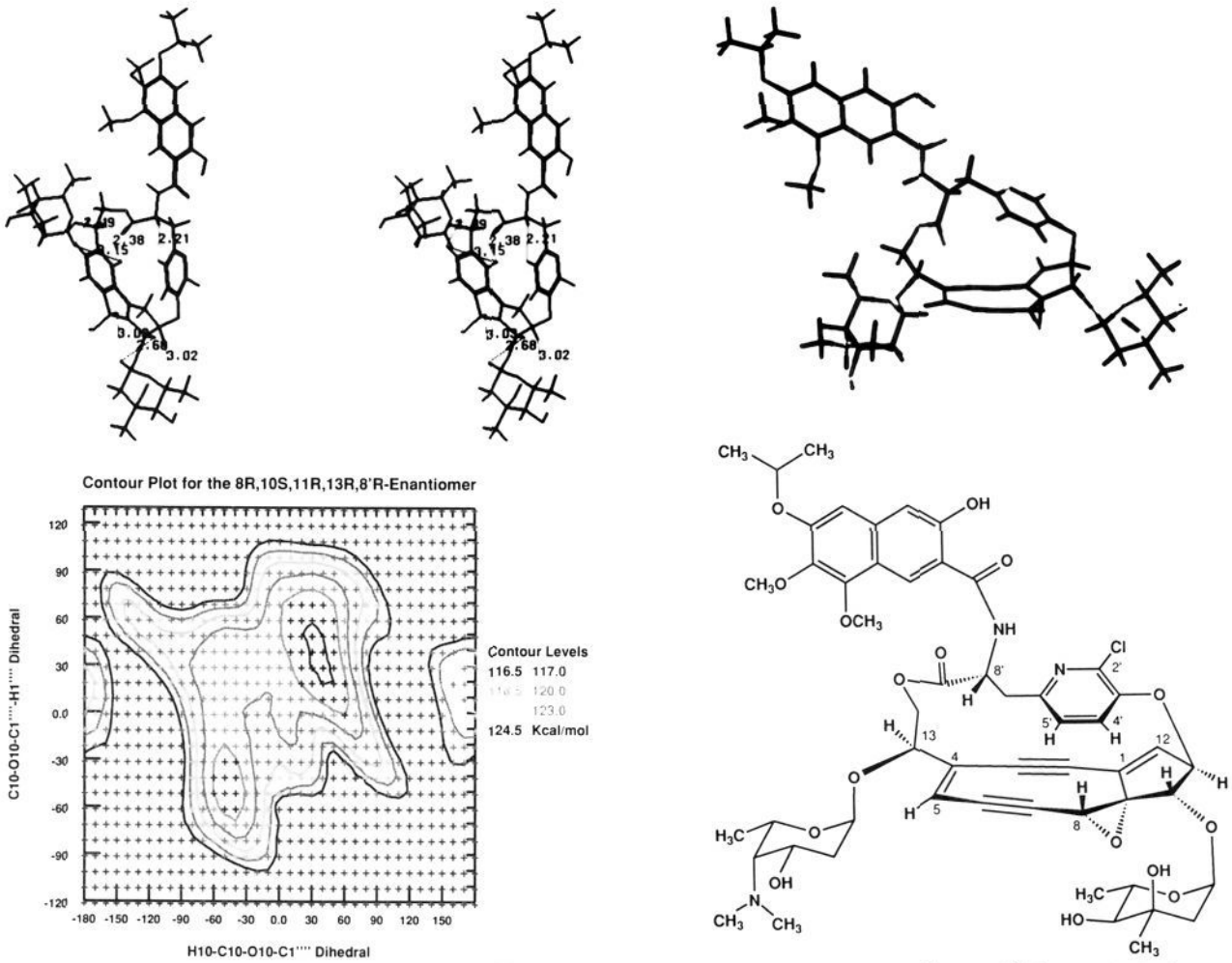

Figure 6. (a, top left) Stereoview (relaxed eye) of the kedarcidin chromophore reduction product (**7a**) showing distances (Å) between key hydrogens. (b, bottom left) Contour plot of the potential energy surface of the kedarcidin chromophore reduction product. The global minimum was found to be at (44.29°, 32.22°). (c, top right) Capstick representation (global minimum) of the kedarcidin chromophore (**1**). (d, bottom right) Perspective drawing of the kedarcidin chromophore.

The global minimum was found to be at (44.29°, 32.22°). All of the conformations in the vicinity of the global minimum allow for the observed H-1'''' to H-8, H-10; and H-5'''' to H-10, H-11 NOE's (i.e. the hydrogen to hydrogen distances fluctuate between 2.2 and 3.5 Å). At the other end of the conformational space (e.g. in the potential energy well around (–40°, –40°)), only the H-1'''' to H-11 NOE is expected. It should be noted that only the observed NOE's between L-mycarose and the aglycone are predicted from the energetically allowed conformations. The opposite enantiomer (8*S*,10*R*,11*S*,13*S*,8'*S*), on the other hand, is inconsistent with the observed NOE's. With this enantiomer, on the basis of the model, H-5'''' is consistently greater than 3 Å from H-8, and H-2b'''' is often within 3 Å of H-11. In summary, the more rigid reduction product (**7a**) was used for predicting absolute stereochemistry from NOE data. To cross validate this prediction, a conformational search of the kedarcidin chromophore (**1**) produced four different minima, all within 6 kcal/mol of the global minimum, which collectively are consistent with the observed NOE data.

On the basis of the observed NOE data and of the model of the sodium borohydride reduction product, the stereochemical assignments of the aglycone centers in the kedarcidin chromophore were inferred to be 8*R*, 9*R*, 10*S*, 11*R*, 13*R*, and 8'*R* (Figure 6c,d). The stereochemistries of centers C-10 and C11 are identical with those of neocarzinostatin; the C-13 stereochemistry is opposite.[5e] Also, the C-8' center of the 2'-chloroazatyrosine portion has the *R* configuration, whereas the same carbon in the antibiotic azatyrosine (**5**) has the *S* configuration.[19]

The mechanism of action of the kedarcidin chromophore (**1**) has been proposed on the basis of sodium borohydride/borodeuteride reduction experiments. Upon sodium borohydride reduction of the chromophore, the olefinic carbon at δ 139.1 (C-12) and its attached proton (δ 6.62) disappeared, with subsequent formation of a new geminal pair (δ 2.40, 2.73). One of the geminal protons (δ 2.40) is shielded by the pyridine ring. Therefore, the second geminal (δ 2.73) proton (selectively replaced by deuterium upon $NaBD_4$ reduction) is trans to the azatyrosine linkage. Inspection of Dreiding models indicates that the chlorine substituent resides directly over C-12 of the parent enediyne, sterically blocking one face. The proposed mechanism thus involves initial attack on the less hindered side of C-12 by the reducing agent, followed by double-bond migration and opening of the epoxide ring. Subsequent cyclization of the enediyne (**13**) gives the 1,4-benzenoid diradical (**14**), the species believed to cause DNA damage (Figure 7). The incorporation of deuterium at C-3 and C-6 in the reduced form (**15**) provides strong support for this hypothesis. Interestingly, the end to end enediyne distances[25] (e.g. C-2 to C-7, Figure 7) as determined by AM1[26] calculations do not change significantly upon epoxide ring opening.

(25) Nicolaou, K. C.; Zuccarello, G.; Ogawa, Y.; Schweiger, E. J.; Kumazawa, T. *J. Am. Chem. Soc.* **1988**, *110*, 4866–4868.

(26) (a) Stewart, J. J. P. MOPAC, A Semi-Empirical Molecular Orbital Program. *QCPE* **1983**, 445. (b) Seiler, F. J. MOPAC 6.0, 1990.

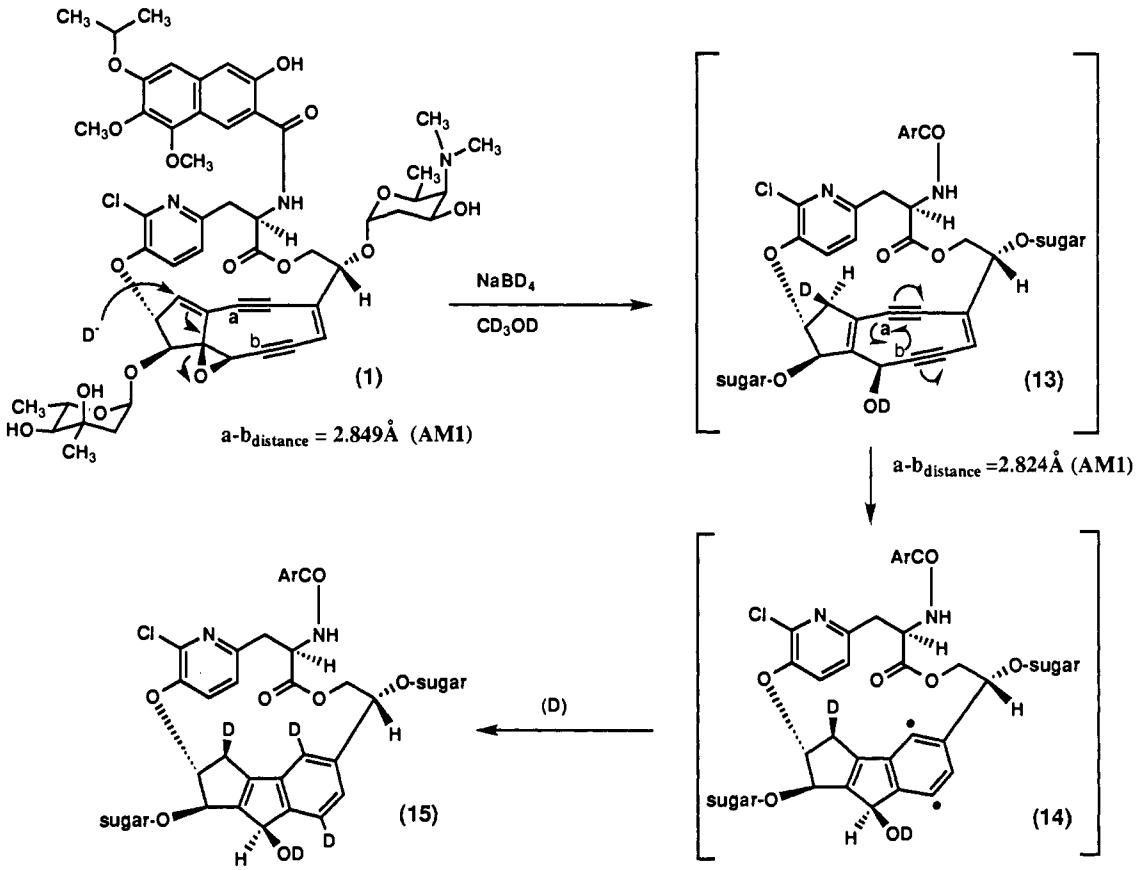

Figure 7. Kedarcidin chromophore (**1**): Proposed mechanism of action as illustrated by $NaBD_4$ reduction.

This would suggest that the opening of the epoxide reduces the strain energy developed in the transition state leading to cycloaromatization.[27] DNA-cleavage experiments[28,29] indicate that the kedarcidin chromophore is also activated by thiols such as β-mercaptoethanol and dithiothreitol. The mechanism of action contrasts with that of the neocarzinostatin chromophore, in which the epoxide ring opening is followed by a cumulene intermediate which subsequently aromatizes to a C-2, C-6 indacene diradical[5a] (i.e. a C_5–C_6–C_5 ring system (neocarzinostatin) vs a C_5–C_5–C_6 (kedarcidin) ring system).

Conclusion

Using a combination of NMR techniques, mass spectrometry, chemical degradation, derivatization, and sodium borohydride reduction experiments, the structure of the kedarcidin chromophore (**1**) was determined. The absolute stereochemistry of the aglycone was inferred by NMR NOE and molecular modeling studies. The chromophore of kedarcidin is a fascinating example of a bioreductively activated DNA-damaging antitumor agent in which the active species is a diradical intermediate. The stereospecific reduction with sodium borodeuteride suggests that the bioreductive events may be stereospecific as well. Preliminary DNA-cleavage studies reveal an unusually high degree of sequence specificity.[28] Molecular modeling and multidimensional NMR studies to determine the solution structure of the intact chromoprotein are in progress. Further studies on kedarcidin's tertiary structure and its mechanism of action will be reported later.

(27) (a) Magnus, P.; Fortt, S.; Pitterina, T.; Snyder, J. P. *J. Am. Chem. Soc.* **1990**, *112*, 4986–4987. (b) Snyder, J. P. *J. Am. Chem. Soc.* **1989**, *111*, 7630–7632.

(28) Zein, N.; Colson, K. L.; Leet, J. E.; Schroeder, D. R.; Solomon, W.; Doyle, T. W.; Casazza, A. M. *Proc. Natl. Acad. Sci. U.S.A.* **1993**, *90*, 2822–2826.

(29) Long, B. H.; Crosswell, A. R.; Casazza, A. M. Unpublished results.

Experimental Section

General. Solvents used for chromatography and chemical modifications were ACS grade and were not redistilled. TLC analyses were carried out using Uniplate Silica Gel GHLF precoated (scored 10 × 20 cm, 0.25 mm) plates. The thin-layer chromatograms were detected with short-wavelength UV light and ceric sulfate and/or vanillin sulfuric acid spray reagents. Preparative TLC separations were performed with E. Merck precoated Silica Gel (Kieselgel 60 F_{254} 20 × 20 cm, 0.5 mm) plates. Vacuum liquid chromatography (VLC) was performed with in-house vacuum, using E. Merck LiChroprep Silica gel 60, 25–40-μm particle size. HPLC analyses were performed using a Rainin C-18 reverse-phase column ("Short-One" 4.6 mm i.d. × 10 cm long, 3-μm particle size, 100-Å pore size) a Waters Associates Model 590 solvent delivery system, and a Hewlett Packard HP-1040A diode array detector.

All ^1H- and ^{13}C-NMR spectra were recorded using a Bruker AM-500 operating at 500.13 and 125.76 mHz, respectively, using a 5-mm broad-banded probe, unless otherwise indicated. Chemical shifts are reported in ppm relative to solvent ($CDCl_3$ δ_H 7.24, δ_C 77.0; DMSO-d_6 δ_H 2.49, δ_C 39.6). Oxygen gas was removed from the NMR sample for NOE analyses by bubbling argon gas through the sample prior to analysis. Spectra were recorded at ambient temperature unless otherwise indicated. UV absorption spectra were determined using a Hewlett Packard 8452A diode array spectrophotometer. IR spectra were obtained on KBr disks using a Perkin-Elmer 1800 Fourier transform spectrometer. Low-resolution mass spectrometric analyses were performed with a Kratos MS50 mass spectrometer and a Finnigan MAT TSQ70 tandem quadrupole mass spectrometer in the positive-ion fast atom bombardment (FAB) mode. The Kratos MS50 instrument was equipped with a saddle-field FAB gun (Ion Tech, Teddington, U.K.) operating at 8 keV with xenon as the primary atom beam. The Finnigan MAT TSQ70 instrument was also equipped with a saddle-field FAB gun (Ion Tech) with the source temperature maintained at 40 °C. Argon was used as the primary particle source as the argon ions were accelerated to 8.0 keV. Small aliquots of sample (≤1 μL) were deposited directly onto the FAB probe tip containing the *m*-nitrobenzyl alcohol (NBA) matrix. Accurate mass measurements were obtained by peak matching on the Kratos MS50 with a cesium iodide saturated glycerol solution as the reference. Subsequent MS/MS substructure analyses were performed with the Finnigan MAT TSQ70

instrument. Argon was used for the MS/MS experiments requiring collisionally activated dissociation (CAD) with an indicated collision gas pressure of 1.0 mTorr. Collision energies of 40–60 eV were used. Full-scan mass spectra were acquired with a 1-s scan rate while MS/MS spectra were acquired with a 1–4-s scan rate.

LC/MS (Thermospray) analyses were obtained using a Finnigan MAT TSQ70 mass spectrometer equipped with a Vestec Model 701A Thermospray LC/MS interface and a Perkin Elmer Series 410 HPLC pump. Direct injection (e.g. no chromatographic separation) of kedarcidin samples was made into the LC/MS source, which was maintained at 250 °C; mobile phase 0.1 M ammonium acetate; flow rate 1.5 mL/min. For samples involving chromatographic separations, the following conditions were used: C-18 reverse-phase HPLC column (Waters NOVAPAK C18, 3.9 × 150 mm); mobile phase 1:1 acetonitrile–0.05 M ammonium acetate buffer, pH 6.8, isocratic; flow rate 1.3 mL/min. Vaporization of the mobile phase was controlled by two thermocouples located at about 10% of the tube length (control temperature) and at the tip of the vaporizing tube (tip temperature). The tip temperature, located in a feedback loop which is used to maintain the control temperature at a preset value,[30] was maintained at 220 °C.

LC/MS Analyses of Kedarcidin. The kedarcidin lot containing three chromophores showed three components of molecular weights 1001, 1015, and 1029 with retention times of 3.3, 5.2, and 6.7 min, respectively. Close inspection of the mass spectra revealed a major thermospray fragment ion from each component as m/z 278, 292, and 306, respectively, differing by subunits of 14 mass units. This corresponds to varying degrees of methylation in the naphthoyl substructure (**9**) (Figure 1). The kedarcidin lot containing one chromophore showed one component of molecular weight 1029 with a 6.7-min retention time. In all cases the apoprotein peak apparently eluted with the void volume, retention time 0.5 min.

Quantitative Determination of Apoprotein–Chromophore Ratios. Using a Hewlett Packard 8452A UV spectrophotometer with Quant II software (curve fitting), the method quantitates the kedarcidin chromophore and apoprotein in the chromoprotein sample using a least-squares best-fit of the first-derivative spectrum over the range 208–360 nm. Standard solutions of apoprotein and chromophore were prepared in 96% water, 4% ethanol, as were several standard mixtures with varying weight ratios. The Quant II software calculates a best-fit spectrum from the standard spectra and extracts the quantitative information from the best-fit spectrum.

Isolation of the Kedarcidin Chromophore (1). The fermentation broth of a novel actinomycete strain (L585-6, ATCC 53650) was prepared as previously described.[10a,13] The raw fermentation broth (700 L) was filtered, adjusted to pH 5.6, and sorbed onto 15 kg of Whatman DE23 anion-exchange resin. The resin was rinsed with six bed volumes of 0.05 M sodium acetate buffer, pH 5.6, followed by elution with 0.5 M sodium chloride in the acetate buffer. This eluate, enriched in kedarcidin, was concentrated and desalted with an Amicon hollow fiber filter unit (10 000 MW cutoff). The >10 000 MW concentrate was lyophilized and used as the starting material in the following extraction step. Typically, a 75-g portion of lyophilized crudes was dissolved in 1 L of water and extracted four times with equal volumes of ethyl acetate, giving 0.34 g of extract. The extract was chromatographed by silica gel vacuum liquid chromatography (2.5 × 11 cm column, 12 g of dry silica gel). Using a step gradient, elution was begun (100 mL each) with benzene, followed by 1% methanol in benzene, 2%, 5%, and 7.5% methanol in benzene (three times). The chromatogram was monitored by TLC (C_6H_6–MeOH, 9:2 v/v). Fractions containing essentially pure chromophore (5–7.5%) were pooled, giving 0.2 g of a buff colored amorphous solid. Special care was taken (e.g. low heat) during the final concentration step to minimize decomposition of the chromophore.

Kedarcidin Chromophore (1): $C_{53}H_{60}N_3O_{16}Cl$; TLC R_f 0.29 (C_6H_6–MeOH, 9:2), 0.16 (C_6H_6–MeOH, 9:1); C-18 HPLC Rt 4.7 min (mobile phase, 1:1 CH_3CN–0.1 M NH_4OAc–AcOH buffer, pH 5.0; flowrate 1.5 mL/min; detector 254 nm); HRFABMS, m/z 1030.3708 ($[M + H]^+$; calcd 1030.3740), 886.2940 ($C_{46}H_{49}N_3O_{13}Cl$), 289.1078 ($C_{16}H_{17}O_5$), 247.0591 ($C_{13}H_{11}O_5$), 158.1178 ($C_8H_{16}NO_2$); IR ν_{max} (KBr) 3432, 2976, 2934, 2832, 2188, 1742, 1656, 1622, 1524, 1470, 1450, 1434, 1386, 1354, 1298, 1240, 1192, 1164, 1114, 1080, 1060, 1032, 1010, 980, 936, 902, 862, 824, 798, 680 cm^{-1}; UV λ_{max} (MeOH) 256, 316 nm (log ϵ 4.78, 4.16). The ^1H and ^{13}C NMR data (DMSO-d_6) appear in Table I.

Methanolysis of the Kedarcidin Chromophore (1). A sample of **1** (0.2 g) was dissolved in approximately 10 mL of methanolic HCl, 4.6 M, and allowed to stand in a sealed vial, under N_2, at room temperature for 64 h. The solution was neutralized with 1 M aqueous sodium bicarbonate and extracted twice with chloroform. The chloroform extract was chromatographed by silica gel VLC (2.5 × 11 cm column), using a dichloromethane–methanol step gradient. Examination of the dichloromethane eluant by TLC ($CHCl_3$–MeOH, 95:5) revealed one major UV quenching zone (254 nm), R_f 0.5, and at least two non-UV quenching components, R_f 0.4 and 0.7, which gave purple-brown coloration upon treatment of the plate with vanillin–sulfuric acid spray reagent with heating. This nonpolar fraction of the methanolysis mixture was used as the starting material in the purification of products **2** and **4**.

Isolation of Methyl α-L-Mycaroside (2). The nonpolar fraction of the crude acidic methanolysis product (100 mg) was chromatographed on a silica gel VLC column (2.5 × 8 cm). Elution was begun with dichloromethane (150 mL), followed by 1%, 2%, 5%, 10%, 15%, and 20% acetone in dichloromethane. TLC (CH_2Cl_2–$(CH_3)_2CO$, 10:2) revealed a single component in the 5% acetone in dichloromethane fraction (8.5 mg), which was identified as methyl α-L-mycaroside (**2**): $C_8H_{16}O_4$; TLC R_f 0.37 (CH_2Cl_2–$(CH_3)_2CO$, 10:2); HRFABMS, m/z 177.1129 ($[M + H]^+$; calcd 177.1127); $[\alpha]_D$ −113° (c, 0.4, $CHCl_3$); ^1H NMR ($CDCl_3$ at 300 MHz) δ 4.74 (1H, dd, J = 3.6, 1.2 Hz, H-1_{eq}), 3.82 (1H, s, C3-OH), 3.60 (1H, dq, J = 9.7, 6.2 Hz, H-5_{ax}), 3.35 (3H, s, H-7), 2.95 (1H, dd, J = 9.7, 11.0 Hz, H-4_{ax}), 2.21 (1H, d, J = 11.0 Hz, C4-OH), 2.02 (1H, dd, J = 1.2, 14.5 Hz, H-2_{eq}), 1.78 (1H, dd, J = 3.6, 14.5 Hz, H-2_{ax}), 1.31 (3H, d, J = 6.2 Hz, H-6), 1.21 (3H, s, H-8); ^{13}C NMR ($CDCl_3$ at 75.5 MHz) δ 98.4 (C-1), 40.7 (C-2), 69.9 (C-3), 76.4 (C-4), 65.5 (C-5), 17.9 (C-6), 55.0 (C-7), 25.7 (C-8).

Isolation of the 2′-Chloroazatyrosyl Naphthoamide Fragment (4). A 300-mg quantity of the nonpolar fraction from the methanolysis mixture was chromatographed using a 2.5 × 11 cm VLC column. Elution (100 mL each) was begun with hexane and hexane–dichloromethane mixtures, followed by dichloromethane and 1% and 2% methanol in dichloromethane. Fractions containing **4** (1% and 2% methanol) were pooled (250 mg) and rechromatographed by silica gel VLC, using hexane–dichloromethane mixtures, followed by 1% methanol in dichloromethane. In this manner 118 mg of **4** was obtained as a white powder: $C_{25}H_{27}N_2O_8Cl$: TLC R_f 0.50 ($CHCl_3$–MeOH, 95:5); HRFABMS, m/z 519.1529 ($[M + H]^+$; calcd 519.1534), 289.1066 ($C_{16}H_{17}O_5$), 247.0591 ($C_{13}H_{11}O_5$), 182.0010 ($C_8H_5NO_2Cl$); IR ν_{max} (KBr) 3364, 2978, 2938, 1738, 1654, 1620, 1566, 1532, 1470, 1434, 1396, 1356, 1332, 1304, 1240, 1196, 1128, 1112, 1080, 1028, 976, 932, 862, 838, 798, 704, 638 cm^{-1}; UV λ_{max} (MeOH) 256, 292, 318 nm (log ϵ 4.78, 4.10, 4.05); ^1H NMR (DMSO-d_6) δ 11.75 (1H, s, br, OH), 10.69 (1H, s br, OH), 9.49 (1H, d, J = 7.9 Hz, NH), 8.56 (1H, s, H-1), 7.34 (1H, d, J = 8.3 Hz, H-4′), 7.30 (1H, d, J = 8.3 Hz, H-5′), 7.12 (1H, s, H-4), 6.97 (1H, s, H-5), 5.52 (1H, dd, J = 7.1, 7.9 Hz, H-8′), 4.75 (1H, septet, J = 6.0 Hz, H-10), 3.98 (3H, s, H-14), 3.80 (3H, s, H-13), 3.58 (3H, s, H-10′), 3.03 (2H, overlapping dd's, J_1 = 6.7, 15.9 Hz, J_2 = 7.1, 15.9 Hz, H-7′), 1.34 (6H, d, J = 6.0 Hz, H-11, H-12); ^{13}C NMR (DMSO-d_6) δ 124.4 (C-1), 116.1 (C-2), 155.0 (C-3), 109.9 (C-4), 134.2 (C-4a), 102.2 (C-5), 153.2 (C-6), 139.0 (C-7), 148.4 (C-8), 117.2 (C-8a), 167.1 (C-9), 70.1 (C-10), 21.8 (C-11, C-12), 60.7 (C-13), 61.5 (C-14), 136.9 (C-2′), 148.9 (C-3′), 124.8 (C-4′), 122.0 (C-5′), 149.8 (C-6′), 38.3 (C-7′), 49.9 (C-8′), 171.1 (C-9′), 51.5 (C-10′).

Isolation of Kedarosamine Methyl Glycoside (3).[17] A sample of the kedarcidin chromophore (**1**) (200 mg) was taken up in 5 mL of methanolic HCl (4.6 M) and allowed to stand at room temperature in a sealed vial for 24 h. The reaction mixture was diluted with 15 mL of water and extracted twice with chloroform. The aqueous phase was adjusted to pH 8–9 upon addition of concentrated ammonium hydroxide and extracted three times with chloroform. The basic organic extract was purified by silica gel preparative TLC using dichloromethane–acetone–ammonium hydroxide, 10:2:0.2, as the developing solvent, yielding 10 mg of a 9:1 anomeric mixture of α- and β-methyl glycosides, respectively. The material was obtained as a volatile oil. α-anomer: $C_9H_{19}NO_3$; TLC R_f 0.60 ($CHCl_3$–MeOH, 95:5); HRFABMS, m/z 190.1439 ($[M + H]^+$; calcd 190.1443); ^1H NMR ($CDCl_3$) δ 4.80 (1H, t, J = 3.2 Hz, H-1), 4.10 (1H, dq, J = 3.3, 7.0 Hz, H-5), 3.93 (1H, dt, J = 5.5, 10.3 Hz, H-3), 3.30 (3H, s, H-7, OMe), 2.59 (6H, s, H-8, H-9, NMe_2), 2.48 (1H, dd, J = 3.3, 5.2 Hz, H-4), 1.90 (1H, ddd, J = 2.6, 5.7, 13.8 Hz, H-2_{eq}), 1.76 (1H, ddd, J = 3.9, 10.4, 13.8 Hz, H-2_{ax}), 1.40 (3H, d, J = 7.0 Hz, H-6, Me); ^{13}C NMR ($CDCl_3$) δ 97.9 (C-1), 35.5 (C-2), 63.3 (C-3), 63.8 (C-4), 67.6 (C-5), 18.0 (C-6), 54.9 (C-7), 44.8 (C-8, C-9).

Synthesis of 2-Chloro-3-hydroxy-6-methylpyridine (6).[18] A 1-g quantity of 3-hydroxy-6-methylpyridine (Aldrich cat. 10,726-3) was dissolved in concentrated HCl (12 M) and warmed to 70 °C. Chlorine gas was bubbled in slowly, with stirring, over a 5-h period. TLC ($CHCl_3$–MeOH, 95:5) after 5 h revealed completion of reaction. The reaction mixture

(30) Vestal, M. L.; Fergusson, G. J. *Anal. Chem.* **1985**, *57*, 2373–2378.

was adjusted to pH 8 upon addition of 1 M sodium bicarbonate and extracted with chloroform. A gray interfacial precipitate formed; this was recovered and recrystallized from methanol–water, 3:2, to give approximately 0.7 g of **6**: C_6H_6NOCl; TLC R_f 0.38 ($CHCl_3$–MeOH, 95:5); HRFABMS, m/z 144.0211 ($[M + H]^+$; calcd 144.0216); ^1H NMR (DMSO-d_6) δ 10.28 (1H, s, C3-OH), 7.21 (1H, d, J = 8.1 Hz, H-4), 7.03 (1H, d, J = 8.1 Hz, H-5), 2.30 (3H, s, Me, H-6); ^{13}C NMR (DMSO-d_6) δ 136.7 (C-2), 147.3 (C-3), 124.6 (C-4), 123.1 (C-5), 147.9 (C-6), 22.5 (C-7). IR ν_{max} (KBr) 3300–2100 br, 1712, 1658, 1612, 1560, 1540, 1498, 1454, 1414, 1320, 1292, 1258, 1226, 1188, 1140, 1094, 1042, 1006, 896, 888, 830, 790, 782, 684. UV λ_{max} (MeOH) 224, 290 nm (log ϵ 3.78, 3.84).

Kedarcidin Chromophore Sodium Borohydride Reduction Product (7a). A sample of the kedarcidin chromophore (**1**), 270 mg, was dissolved in 20 mL of methanol. Excess sodium borohydride (approximately 50 mg) was added slowly, with stirring, at room temperature over a 2-h period. Vigorous bubbling and a color change from dark-red to yellow-orange was observed upon addition of reducing agent. TLC ($CHCl_3$–MeOH, 85:15) after 2 h revealed total consumption of starting material. The reaction mixture was evaporated to near dryness and partitioned between water (pH 7) and chloroform. The chloroform extract was purified by silica gel VLC (2.5 × 7 cm column). Elution was begun (100 mL each) with chloroform, followed by 2%, 4%, 2 × 6%, 8%, and 10% methanol in chloroform. The chromatogram was followed by TLC ($CHCl_3$–MeOH, 85:15). The 6–10% methanol fractions were combined and purified by silica gel preparative TLC, using the same solvent, to give 81 mg of reduction product **7a**. For reduction with sodium borodeuteride, the same general procedure was used, using methanol or deuterated methanol (d_4) as reaction solvent. Reduction product **7a**: $C_{53}H_{64}N_3O_{16}Cl$; TLC R_f 0.57 ($CHCl_3$–MeOH, 85:15), 0.1 ($CHCl_3$–MeOH, 95:5); HRFABMS, m/z 1034.4021 ($[M + H]^+$; calcd 1034.4053); UV λ_{max} (MeOH) 232, 258, 304 nm (log ϵ 4.69, 4.79, 4.11); IR ν_{max} (KBr) 3440, 2974, 2934, 1742, 1656, 1622, 1524, 1470, 1452, 1434, 1386, 1354, 1332, 1242, 1192, 1162, 1122, 1082, 1056, 1026, 902. The ^1H and ^{13}C NMR data ($CDCl_3$) appear in Table II. Sodium borodeuteride–methanol major product: $C_{53}H_{63}DN_3O_{16}Cl$; HRFABMS, m/z 1035.4085 ($[M + H]^+$; calcd 1035.4116). Sodium borodeuteride–methanol-d_4 product: $C_{53}H_{61}D_3N_3O_{16}Cl$: HRFABMS, m/z 1037.4210 ($[M + H]^+$; calcd 1037.4242).

Acetylation of Reduced Kedarcidin Chromophore (7a). A 31-mg sample of reduced kedarcidin chromophore (**7a**) was dissolved in 5 drops of pyridine, and to the solution was added 15 drops of acetic anhydride. The contents were allowed to stand at room temperature for 24 h. The reaction mixture was evaporated to dryness and purified by preparative TLC using benzene–methanol, 9:1, as developing solvent, giving 17 mg of a tetraacetate ester **7b**: $C_{61}H_{72}N_3O_{20}Cl$; TLC R_f 0.78 ($CHCl_3$–MeOH, 95:5); HRFABMS, m/z 1202.4492 ($[M + H]^+$; calcd 1202.4476). The ^1H and ^{13}C NMR data ($CDCl_3$) appear in Table III.

Methanolysis of Reduced Kedarcidin Chromophore (7a). A 50-mg sample of reduced kedarcidin chromophore (**7a**) was dissolved in 0.5 mL of methanol, and to the solution was added 0.6 mL of methanolic HCl (4.2 M). TLC ($CHCl_3$–MeOH, 85:15) after 24 h revealed total consumption of starting material. Workup and preparative TLC ($CHCl_3$–MeOH, 85:15) yielded 3.1 mg of the aglycone (**12**): $C_{40}H_{43}N_2O_{12}Cl$; TLC R_f 0.37 ($CHCl_3$–MeOH, 9:1); HRFABMS, m/z 817.2155 ($[M + K]^+$; calcd 817.2142), 517.1392 ($C_{25}H_{26}N_2O_8Cl$), 289, 247; ^1H NMR ($CDCl_3$) δ 8.24 (1H, s, H-1″), 8.05 (1H, d, J = 8.2 Hz, NH), 7.47 (1H, d, J = 7.6 Hz, H-6), 7.41 (1H, d, J = 8.4 Hz, H-4′), 7.35 (1H, d, J = 8.4 Hz, H-5′), 7.21 (1H, d br, J = 7.6 Hz, H-5), 7.15 (1H, s br, H-3), 7.08 (1H, s, H-4″), 6.69 (1H, s, H-5″), 5.65 (1H, m, H-8′), 5.17 (1H, s br, H-8), 5.12 (1H, m, H-11), 4.82 (1H, m, H-10), 4.80 (1H, m, H-13), 4.70 (1H, sept, J = 6.0 Hz, H-10″), 4.11 (3H, s, OMe, H-14″), 3.87 (3H, s, OMe, H-13″), 3.70 (3H, s, COOMe), 3.70 (1H, m, H-14a), 3.61 (1H, m, H-14b), 3.54 (3H, s, C-8 or C-13 OMe), 3.20 (1H, m, H-12a), 3.17 (1H, dd, J = 5.0, 16.0 Hz, H-7′a), 2.97 (1H, dd, J = 6.9, 16.0 Hz, H-7′b), 2.60 (1H, d br, J = 17.4 Hz, H-12b), 1.43 (6H, d, J = 6.0 Hz, H-11″ and H-12″ Me).

Molecular Mechanics Calculations. The modeling studies were conducted with Molecular Simulations[31] Quanta/CHARMM software (version 3.1) running on an IBM Risk 6000/540 workstation. A distance-dependent dielectric was used to approximate electrostatic screening due to solvent. The nonbonded vswitch and shift smoothing functions were used to smooth the Van der Waals and electrostatic interactions, respectively, to zero between 10.5 and 14.5 Å with a 15.50-Å cutlist.[32] All energy minimizations were minimized to a RMS gradient force of ≤0.100 with the adopted-basis Newton Raphson minimizer.[24] In the grid search, the grid was scanned ±180° in 10-deg increments from a reference point in which the two dihedrals being searched were set to zero. At each point in the grid the dihedrals were fixed and the conformation was minimized.

Acknowledgment. The authors thank K. S. Lam, D. R. Gustavson, S. Forenza, and the NCI–Frederick Cancer Research and Development Center for fermentation support; S. W. Mamber, K. W. Brookshire, and A. R. Crosswell for bioassay guidance; and R. A. Dalterio, E. H. Kerns, K. J. Volk, and C. F. Piccirillo for analytical support. The authors thank N. Zein for helpful discussions.

(31) Molecular Simulations Inc., 200 Fifth Avenue, Waltham, MA 02254.
(32) Loncharich, R. J.; Brooks, B. R. *Proteins: Struct., Funct., Genet.* **1989**, *6*, 46–60.